Analytical Simplification of the 2-D Method of Moments Impedance Integral

Jerry R. Smith, Jr., *Member, IEEE,* and Mark S. Mirotznik, *Member, IEEE*

***Abstract*—The elements of the two-dimensional (2-D), method of moments (MoM) impedance matrix are analytically reduced by way of an integral transform. The resulting impedance expression is a single integral with an analytic integrand for nearly arbitary shape and weight function sets. The reduced expression requires fewer computations, thereby reducing the matrix fill time. This moments via integral transform method (MITM) is based on an integral representation of the Green's function (Hankel function) and utilizes a special integral transform. The method is developed for 2-D perfectly electrically conducting bodies subjected to a transverse magnetic field. A comparison between brute force and MITM is presented for polynomial shape and weight functions.**

***Index Terms*—Electromagnetic scattering, method of moments (MoM), transforms.**

I. Introduction

THE fill time of the impedance matrix represents a significant choke-point in method of moments (MoM) calculations because the matrix elements are expressed as multidimensional integrals. Numerical evaluations are computationally expensive and are often difficult at higher frequencies. Previous efforts to reduce the matrix fill time employed spectral domain representations of the Green's function. DiPerna and Feit [1] used the spectral domain representation in conjunction with a rational function approximation of the Green's function to reduce the matrix fill time. Similarly, Aksun *et al.* [2] developed a numerically efficient spectral domain methods for two-dimensional (2-D) stratified media, and Heckmann and Dvorak [3] developed a closed-form expression for the impedance of shielded components based on a series of incomplete Lipschitz–Hankel integrals also by solution in the spectral domain. Finally, Alatan *et al.*, [4] approximated the spatial domain impedance terms by using a spectral domain approximation of the three-dimensional (3-D) Green's function. This method analytically evaluates the impedances for polynomial shape and weight functions.

The contribution of this paper is to analytically reduce the 2-D MoM impedance expression from a double integral to a single integral for nearly arbitary shape and weight function sets without inherent approximations. This is done entirely in the spatial domain by utilizing an integral expression of the free-space Green's function, and the resulting simplification reduces the fill times of the MoM impedance matrix.

Section II presents the MoM system of equations and the impedance for 2-D linear elements. Section III presents integral represention of the Green's function. Section IV uses these integral representations within the impedance expression, and the resulting triple integral is analytically reduced to a single integral by making use of a specialized integral transform defined in Section IV. Section V compares the accuracy and speed of the brute force and moments via integral transform method (MITM) evaluations of the MoM impedance terms. Conclusions and final comments are contained in Section VI.

Manuscript received September 25, 2003; revised November 20, 2003. This work was supported by the Naval Surface Warfare Center, Carderock Division Intra-Laboratory Independent Research Board.

J. R. Smith, Jr., is with the Naval Surface Warfare Center, Carderock Division, West Bethesda, MD 20817-5700 USA (e-mail: smithjr@nswccd.navy.mil).

M. S. Mirotznik is with the Naval Surface Warfare Center, Carderock Division, West Bethesda, MD 20817-5700 USA and the Electrical Engineering Department, The Catholic University of America, Washington, DC 20017 USA.

Digital Object Identifier 10.1109/TAP.2004.835164

II. Method of Moments Solution

The electric field integral equation (EFIE) for a 2-D, perfectly electrically conducting (PEC) body defined by the contour C and subjected to an incident TM field, is given by [5, pg. 150, (3.86)][1]

$$E_z^{\text{inc}}(\boldsymbol{\rho} \in C) = \frac{\omega\mu}{4} \int_C H_0^{(1)}(\kappa|\boldsymbol{\rho} - \boldsymbol{\rho}'|) J(\boldsymbol{\rho}')\, dC' \quad (1)$$

where $H_0^{(1)}$ is the Hankel function of the first kind, the wave number is $\kappa = 2\pi/\lambda$, the incident electric field E_z^{inc} only has a z component, and the surface current is denoted by J. The scatterer C is partioned into P nonoverlapping elements with the surface current distribution $J_p(\boldsymbol{\rho})$. These surface currents are expanded in terms of the set of shape functions $S_{pm}(\boldsymbol{\rho})$, which are zero everywhere *except* on the pth element. Finally, taking the inner product with a set of weight functions $W_{qn}(\boldsymbol{\rho})$, which are zero everywhere *except* on the qth element, yields the MoM system of equations

$$V_{qn} = \sum_{p=1}^{P} \sum_{m} Z_{qn,pm} \mathcal{A}_{pm} \quad (2)$$

where the excitation voltages are given by

$$V_{qn} \equiv \int_{C_q} W_{qn}(\boldsymbol{\rho}_q) E_z^{\text{inc}}(\boldsymbol{\rho}_q) dC_q \quad (3)$$

the unknown amplitude of the mth mode on the pth element is $\mathcal{A}_{pm}$, and the impedance between the mth mode on the pth element and the nth mode on the qth element is given by

$$Z_{qn,pm} \equiv \frac{\omega\mu}{4} \int_{C_q} \int_{C_p} H_0^{(1)}(\kappa|\boldsymbol{\rho}_q - \boldsymbol{\rho}_p'|) \times W_{qn}(\boldsymbol{\rho}_q) S_{pm}(\boldsymbol{\rho}_p')\, dC_p' dC_q. \quad (4)$$

[1]The form presented here uses $H_0^{(1)}(\kappa|\boldsymbol{\rho} - \boldsymbol{\rho}'|)$ as the Green's function, which is due to the authors' preference in sign convention. A detailed discussion of the MoM is found in [5, ch. 4]

A. The General Polar Distance Equation

If body C is partioned into linear elements, then the position of any point $s_p \in [0,1]$ on the pth linear element is given by

$$\boldsymbol{\rho}_p(s_p) = \boldsymbol{\rho}_p^0 + s_p L_p \hat{\mathbf{l}}_p \tag{5}$$

where L_p is the length of the pth element and $\hat{\mathbf{l}}_p$ is the unit vector along the pth element from the starting node at $\boldsymbol{\rho}_p^0 = x_p^0\hat{\mathbf{e}}_x + y_p^0\hat{\mathbf{e}}_y$ to the ending node point at $\boldsymbol{\rho}_p^0 + L_p\hat{\mathbf{l}}_p$. The distance between any two points $\Delta_{p,q}(s_p, s_q) = |\boldsymbol{\rho}_q(s_q) - \boldsymbol{\rho}_p'(s_p)|$ is given by (6) at the bottom of the page, where the constant σ_p^x is the projection of the pth element onto the x-axis ($\sigma_p^x = \hat{\mathbf{e}}_x \cdot \hat{\mathbf{l}}_p$), similarly for σ_p^y. Defining the linear functions $\Lambda_1(s_p, s_q) \equiv A_p s_p + B_q s_q + C_{pq}$ and $\Lambda_2(s_p, s_q) \equiv D_p s_p + E_q s_q + F_{pq}$, which are related to the horizontal distances $\Delta x(s_p, s_q)$ and vertical distances $\Delta y(s_p, s_q)$ between the test and weight sample points, yields

$$\Delta_{p,q}(s_p, s_q) = \sqrt{\Lambda_1^2(s_p, s_q) + \Lambda_2^2(s_p, s_q)}. \tag{7}$$

Using (7), the impedance integral (4) becomes

$$\begin{aligned} Z_{qn,pm} = \frac{\omega\mu L_p L_q}{4} &\int_{s_q=0}^{s_q=1} W_{qn}(s_q)\, ds_q \\ &\times \int_{s_p=0}^{s_p=1} S_{pm}(s_p) \\ &\times H_0^{(1)}\left(\kappa\sqrt{\Lambda_1^2(s_p, s_q) + \Lambda_2^2(s_p, s_q)}\right) ds_p. \end{aligned} \tag{8}$$

Section IV will develop an analytical method to simplify (8) into a single integral.

III. Integral Representations of the Green's Function

This section presents and discusses integral representations of the Green's function that will be used in Section IV to simplify (8).

A. Integral Representation for Distinct Element Case ($p \neq q$)

Erdélyi *et al.* [6, p. 283, (5.16.46)] give the Laplace transform, for $g \geq 0$

$$\begin{aligned} \sqrt{\frac{2}{\pi}}\frac{1}{\xi^\nu} e^{\beta g} K_\nu(\beta\xi) = a^{\frac{1}{2}-\nu}\beta^{-\nu} &\int_0^\infty e^{-gt}(t^2 + 2\beta t)^{\frac{1}{2}\nu - \frac{1}{4}} \\ &\times J_{\nu-\frac{1}{2}}(a\sqrt{t^2 + 2\beta t})\, dt \end{aligned} \tag{9}$$

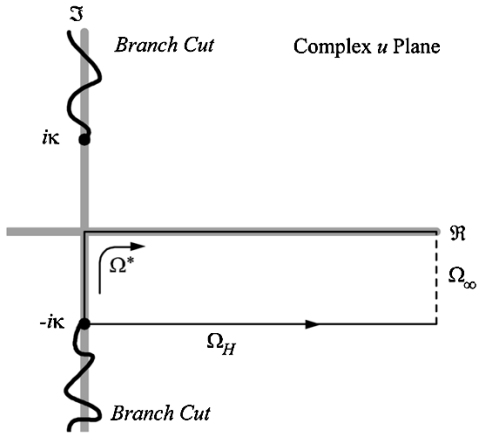

Fig. 1. Complex u-plane paths of integration for (10) and (11).

with the constraints $\mathrm{Re}(\nu) > -(1/2)$ and $|\arg\beta| < \pi$, where $\xi \equiv \sqrt{g^2 + a^2}$, $K_\nu(z)$ is the Bessel function of an imaginary argument and $J_\mu(z)$ is the μth-order Bessel function of the first kind. This yields, for $\nu = 0$, the integral representation of the Green's function

$$\begin{aligned} H_0^{(1)}(\kappa\sqrt{g^2 + a^2}) = \frac{2}{i\pi} &\int_{-i\kappa}^{\infty - i\kappa} \\ &\times \frac{e^{-|g|u}\cos(a\sqrt{u^2 + \kappa^2})}{\sqrt{u^2 + \kappa^2}}\, du. \end{aligned} \tag{10}$$

Equation (10) was derived by using the expression for the fractional order Bessel function [7, p. 966, (8.464.2)], the relationship between $K_0(z)$ and the Hankel function of the first kind $H_0^{(1)}(z)$ [7, p. 952, (8.407.1)], substituting $\beta = -i\kappa$, and changing the variable of integration to $u = t - i\kappa$.

The two branch points at $u = \pm i\kappa$ in (10) and the corresponding semi-infinite branch cuts (Fig. 1) are a result of the $\sqrt{u^2 + \kappa^2}$ terms. For large κ, numerically evaluating (10) along Ω_H is difficult because the oscilliation amplitudes are very large. Using the Cauchy–Goursat theorem [8, p. 327)], the integral path can be transformed.[2] In particular, choosing the closed contour $\Omega = \Omega_H + \Omega_\infty - \Omega^*$ where Ω_∞ is the path from $\infty - i\kappa$ to ∞ and the contour Ω^* is the two part path from $-i\kappa$ through zero to ∞ (see Fig. 1). There are no poles within this contour and the integral along the contour Ω_∞ is zero. Therefore, a generally more stable alternate integral equivalent for (10) is

$$H_0^{(1)}(\kappa\sqrt{g^2 + a^2}) = \frac{2}{i\pi}\int_{\Omega^*} \frac{e^{-|g|u}\cos(a\sqrt{u^2 + \kappa^2})}{\sqrt{u^2 + \kappa^2}}\, du. \tag{11}$$

Equation (11) will be used in evaluating the distinct element impedances.

[2]The transformed path cannot cross a branch cut but can come arbitrarily close to a branch point. Branch cuts of the type in (10) can also be transformed into a finite cut connecting the branch points [8, pp. 321–322].

$$\Delta_{p,q}(s_p, s_q) = \sqrt{\left(x_p^0 + s_p L_p \sigma_p^x - x_q^0 - s_q L_q \sigma_q^x\right)^2 + \left(y_p^0 + s_p L_p \sigma_p^y - y_q^0 - s_q L_q \sigma_q^y\right)^2} \tag{6}$$

B. Integral Representation for Self-Element Case ($p = q$)

Another integral representation of $H_0^{(1)}(z)$ for $\mathrm{Re}(z) > 0$ is given by Gradshteyn *et al.* [7, p. 957, (8.423.1)][3]

$$H_0^{(1)}(z) = \frac{2}{\pi}\int_{\Gamma} e^{iz\cos\phi}d\phi \tag{12}$$

where the contour Γ goes from zero to $\pi/2$ to $\pi/2 - i\infty$. This integrand contains no poles and will be used in evaluating the self-element impedances.[4]

IV. Simplification of the Impedance Integral

This section develops the analytical simplification of the general impedance integral (8) based on the integral $\mathcal{R}$ transformation. The $\mathcal{R}$ transform, with kernel $\mathcal{K}(x,u)$ acting on a function $F(x)$, is defined as

$$\mathcal{R}\{F(x);\mathcal{K}(x,u);[a,b]\} \equiv \int_{x=a}^{x=b} F(x)e^{-\mathcal{K}(x,u)x}\,dx. \tag{13}$$

The function $\mathbf{F}(u;\alpha,\beta,\kappa)$ represents the $\mathcal{R}$ transformation of $F(x)$ for the kernel $r(u;\alpha,\beta,\kappa) \equiv \alpha u + i\beta\sqrt{u^2+\kappa^2}$.

A. The Distinct Element ($p \neq q$) Integral Simplification

Using (10), the general impedance integral (8) expands to

$$\begin{aligned} Z_{qn,pm} = \frac{\mu\omega L_p L_q}{4\pi i}\int_{\Omega^*}\frac{e^{-C_{pq}u}du}{U(u)} &\times \int_{s_p=0}^{s_p=1} S_{pm}(s_p)e^{-A_p s_p u}ds_p \\ &\times \int_{s_q=0}^{s_q=1} W_{qn}(s_q)e^{-B_q s_q u}ds_q \\ &\times \Big[e^{iD_p s_p U(u)}e^{iE_q s_q U(u)}e^{iF_{pq}U(u)} \\ &+e^{-iD_p s_p U(u)}e^{-iE_q s_q U(u)}e^{-iF_{pq}U(u)}\Big] \end{aligned} \tag{14}$$

for $\Lambda_1(s_p,s_q) > 0$ with $U(u) \equiv \sqrt{u^2+\kappa^2}$.

For the kernel $\mathcal{K}(x,u) = r(u;\alpha,\beta,\kappa) \equiv \alpha u + i\beta\sqrt{u^2+\kappa^2}$, the $\mathcal{R}$ transform (13) becomes

$$\begin{aligned} \mathbf{F}[u;\alpha,\beta,\kappa] &= \mathcal{R}\{F(x);r(u;\alpha,\beta,\kappa);[0,1]\} \\ &= \int_{s=0}^{s=1} F(s)e^{-\alpha s u - i\beta s\sqrt{u^2+\kappa^2}}\,ds. \end{aligned} \tag{15}$$

For the distinct element case ($p \neq q$) with $\Lambda_1(s_p,s_q) > 0$, the impedance integral (14) reduces to

$$Z_{qn,pm} = \frac{\mu\omega L_p L_q}{4\pi i}\int_{\Omega^*}\frac{\mathbf{I}^{(1)}_{qn,pm}[u] + \mathbf{I}^{(2)}_{qn,pm}[u]}{\sqrt{u^2+\kappa^2}}\,du \tag{16}$$

[3]The form presented differs by changing the variable ($\phi = \theta + \pi/2$), reversing the contour's direction, and utilizing the integrand's symmetry.

[4]Zhang [9] proposed (12) to evaluate the self-impedance for the modal expansion method.

in terms of the transformed functions

$$\begin{aligned} \mathbf{I}^{(1)}_{qn,pm}[u] &\equiv \mathbf{S}_{pm}[u;A_p,D_p,\kappa]\mathbf{W}_{qn}[u;B_q,E_q,\kappa] \\ &\quad\times\exp[-C_{pq}u - iF_{pq}U(u)] \end{aligned} \tag{17}$$

$$\begin{aligned} \mathbf{I}^{(2)}_{qn,pm}[u] &\equiv \mathbf{S}_{pm}[u;A_p,-D_p,\kappa]\mathbf{W}_{qn}[u;B_q,-E_q,\kappa] \\ &\quad\times\exp[-C_{pq}u + iF_{pq}U(u)] \end{aligned} \tag{18}$$

which are defined using (15).

1) Transformation of Element Pairs: The requirement $\Lambda_1(s_p,s_q) > 0$ in (16) ensures that the integrand converges to zero as $|u| \to \infty$. Since $\Delta_{p,q}(s_p,s_q)$ depends only on the relative positions and orientations of the pth and qth elements, the geometric coefficients $A_p, B_q, C_{pq}, D_p, E_q$, and F_{pq} can be transformed by a local coordinate system translation and rotation [10]. Furthermore, the starting and ending nodes of each element, as well as the elements themselves, may be interchanged.[5] These transformations allow most element configurations to meet the $\Lambda_1(s_p,s_q) > 0$ requirement.[6]

B. The Self-Element ($p = q$) Integral Simplification

For the self-element case ($p = q$), the distance (7) simplifies to

$$\Delta_{p,p}(s_p,s_q) = L_p|s_p - s_q| \tag{19}$$

yielding the self-element impedance integral

$$\begin{aligned} Z_{pn,pm} \equiv \frac{\omega\mu L_p^2}{4}\int_{s_q=0}^{s_q=1} W_{pn}(s_q)ds_q \int_{s_p=0}^{s_p=1} S_{pm}(s_p)ds_p \\ \times H_0^{(1)}(\kappa L_p|s_p - s_q|) \end{aligned} \tag{20}$$

which, by using (12), simplifies to

$$\begin{aligned} Z_{pn,pm} \equiv \frac{\omega\mu L_p^2}{2\pi}\int_{s_q=0}^{s_q=1} W_{pn}(s_q)ds_q \int_{s_p=0}^{s_p=1} S_{pm}(s_p)ds_p \\ \times \int_{\Gamma} e^{i\kappa L_p|s_p - s_q|\cos\phi}d\phi. \end{aligned} \tag{21}$$

The self-impedence ($p = q$) reduces to

$$Z_{pn,pm} = \frac{\omega\mu L_p^2}{2\pi}\int_{\Gamma}\left\{\mathbf{W}^{S1}_{n\,|\,pm}[\phi] + \mathbf{W}^{S2}_{n\,|\,pm}[\phi]\right\}d\phi \tag{22}$$

where the transformed functions

$$\mathbf{S}^{S1}_{pm}[x] \equiv \mathcal{R}\{S_{pm}(y);\varrho(\phi);[0,x]\} \tag{23}$$

$$\mathbf{S}^{S2}_{pm}[x] \equiv \mathcal{R}\{S_{pm}(y);-\varrho(\phi);[x,1]\} \tag{24}$$

$$\mathbf{W}^{S1}_{n\,|\,pm}[\phi] \equiv \mathcal{R}\left\{W_{pn}(x)\mathbf{S}^{S1}_{pm}(x);-\varrho(\phi);[0,1]\right\} \tag{25}$$

$$\mathbf{W}^{S2}_{n\,|\,pm}[\phi] \equiv \mathcal{R}\left\{W_{pn}(x)\mathbf{S}^{S2}_{pm}(x);\varrho(\phi);[0,1]\right\}. \tag{26}$$

are defined in terms of the general $\mathcal{R}$ transform (13) with kernel $\mathcal{K}(x,\phi) = \varrho(\phi) \equiv i\kappa L_p\cos\phi$.

[5]Interchanging the elements is equivilent to interchanging the geometric coefficients $A_p \rightleftharpoons B_q$ and $D_p \rightleftharpoons E_q$.

[6]Equations (17) and (18) can be recast with a $\Lambda_2(s_p,s_q) > 0$ requirement.

The term $|s_p - s_q|$ in (21) requires that the innermost integral be divided into two domains: $D_1\{s_p \in [0, s_q]\}$ and $D_2\{s_p \in [s_q, 1]\}$. The scripts of $\mathbf{S}^{S1}_{pm}(x)$ denote that the mth mode of the shape function on the pth element was in the innermost integral and that the transform was over D_1. Similarly, the scripts of $\mathbf{W}^{S1}_{n\,|\,pm}(x)$ denote that the nth mode of the weight function was transformed along with $\mathbf{S}^{S1}_{pm}(x)$.

If the order of integration is exchanged in (21), the self-element impedance integral reduces to

$$Z_{pm,pm} = \frac{\omega\mu L_p^2}{2\pi}\int_\Gamma \left\{\mathbf{S}^{W1}_{m\,|\,pn}[\phi] + \mathbf{S}^{W2}_{m\,|\,pn}[\phi]\right\} d\phi \tag{27}$$

where the transformed functions have definitions similar to (23)–(26).

C. $\mathcal{R}$ Transformation of Polynomial Functions

The polynomial shape and weight function sets are

$$S_{pm}(s_p) = s_p^m \tag{28}$$
$$W_{qn}(s_q) = s_q^n \tag{29}$$

for $m \geq 0$. In terms of the transformation variable

$$r(u; A_p, \pm D_p, \kappa) = A_p u \pm i D_p\sqrt{u^2 + \kappa^2} \tag{30}$$

the transformed shape functions $\mathbf{S}_{pm}[u] \equiv \mathbf{S}_{pm}(u; A_p, \pm D_p, \kappa)$ are then given by the recursion relationships for $p \neq q$

$$\mathbf{S}_{p0}[u] = \frac{1 - e^{-r}}{r} \quad \text{for } m = 0 \tag{31}$$
$$\mathbf{S}_{pm}[u] = \frac{m\mathbf{S}_{p(m-1)}[u] - e^{-r}}{r} \quad \text{for } m > 0. \tag{32}$$

The transformed weight function $\mathbf{W}_{qn}[u] \equiv \mathbf{W}_{qn}(u; B_q, \pm E_q, \kappa)$ also obeys (31) and (32).

For the self-element case ($p = q$), the transformation variable is

$$\varrho(\phi) = i\kappa L_p \cos\phi. \tag{33}$$

Defining the transformed function $\mathbf{W}^{\pm\varrho}_{pn}[\phi] \equiv \mathcal{R}\{W_{pn}(x); \pm\varrho(\phi); [0, 1]\}$, the self-element transformed functions for $m = 0$ are

$$\mathbf{W}^{S1}_{n\,|\,p0}[\phi] = \frac{(n+1)\mathbf{W}^{-\varrho}_{pn}[\phi] - 1}{(n+1)\varrho} \tag{34}$$
$$\mathbf{W}^{S2}_{n\,|\,p0}[\phi] = \frac{e^{\varrho}(n+1)\mathbf{W}^{+\varrho}_{pn}[\phi] - 1}{(n+1)\varrho}. \tag{35}$$

For $m > 0$, the recursion relationships for the self-element transformed functions are

$$\mathbf{W}^{S1}_{n\,|\,pm}[\phi] = \frac{m(m+n+1)\mathbf{W}^{S1}_{n\,|\,p(m-1)}[\phi] - 1}{(m+n+1)\varrho} \tag{36}$$
$$\mathbf{W}^{S2}_{n\,|\,pm}[\phi] = \frac{1 + m(m+n+1)\mathbf{W}^{S2}_{n\,|\,p(m-1)}[\phi]}{-(m+n+1)\varrho} + \frac{e^{\varrho}}{\varrho}\mathbf{W}^{+\varrho}_{pn}[\phi]. \tag{37}$$

TABLE I
COORDINATES OF ELEMENT NODES

	Element p	Element q
Case 1	$(0, 0)$ to $(1, 0)$	$(2, 1)$ to $(3, 2)$
Case 2	$(0, 0)$ to $(1, 0)$	$(0, 0)$ to $(1, 0)$

V. NUMERICAL EVALUATION OF THE IMPEDANCE

This section presents numerical comparisons between the general impedance (8) and the MITM integrals (16) and (22) for polynomial shape and weight function sets. Comparison of the compution times are included.

A. Comparison of Brute Force and MITM

Calculations of the impedance $Z_{qn,pm}$ using brute force evaluation of (8) and evaluating the MITM integral (16) are presented to demonstrate convergence for a wide range of wave numbers κ. The brute force evaluations of (8) used a Simpson's rule [11] integration scheme with $\lambda/40$ sampling. The evaluations of (16) also used a Simpson's rule with approximately $10^3 L_p/\lambda$ samples for the finite path and $10^2 L_p/\lambda$ samples for the infinite path. Although part of Ω^* in (16) is infinite, the integrand approaches zero exponentially, allowing the integration to be truncated[7] around $u = 5.0L_p/\lambda$. A small value $\epsilon = 10^{-6}$ was added to the singular arguments of the Hankel function in (8) and to the denominator of (16) to avoid the singularities.

For the self-elements, evaluation of (27) used a Simpson's rule with 10^4 samples for both the finite and the infinite paths; the infinite path in (27) was truncated at $u = 10$. The transformed polynomial functions (34)–(37) are singular at the turning point $\phi = (\pi/2)$. Since (12) contains no poles in the ϕ plane, the contour path Γ can be deformed to *cut around* $\phi = (\pi/2)$. The self-element calculations presented used this technique. Note that the brute force evaluation of (8) for the self-patch becomes increasingly difficult for small λ and that $\epsilon = 10^{-7}$ was required for convergence at $L_p/\lambda = 10$.

Convergence of the method is shown for two cases. `Case 1` consists of two distinct elements while `Case 2` is a self-element case. Since all element configurations can be rotated and translated, we present cases where the p element is of unit length, oriented along the x-axis, and starting at the origin. Table I details the element nodes of the two cases. Note that `Case 2` (self-element) is a singular case because $\Delta_{pq}(s_p, s_q) = 0$ within the domain of integration. For both cases, impedance calculations for polynomial shape and weight functions are presented and the impedances are normalized by $4/\mu\omega L_p L_q$.

1) `Case 1`*—Distinct Elements:* Fig. 2 plots the scaled impedance for $S_{p1}(s_p) = s_p$ and $W_{q2}(s_q) = s_q^2$. The impedances calculated by (8) and (16) are virtually identical. Similar convergences were obtained for different element configurations including elements sharing a common node.

2) `Case 2`*—Self-Element:* Fig. 3 plots the scaled impedance for $S_{p1}(s_p) = s_p$ and $W_{q2}(s_q) = s_q^2$. The impedances calculated by (8) and (27) are virtually identical.

[7]At $u = 5.0L_p/\lambda$, the exponentially decaying integrand is on the order of 10^{-10} or smaller so truncation error was neglectable.

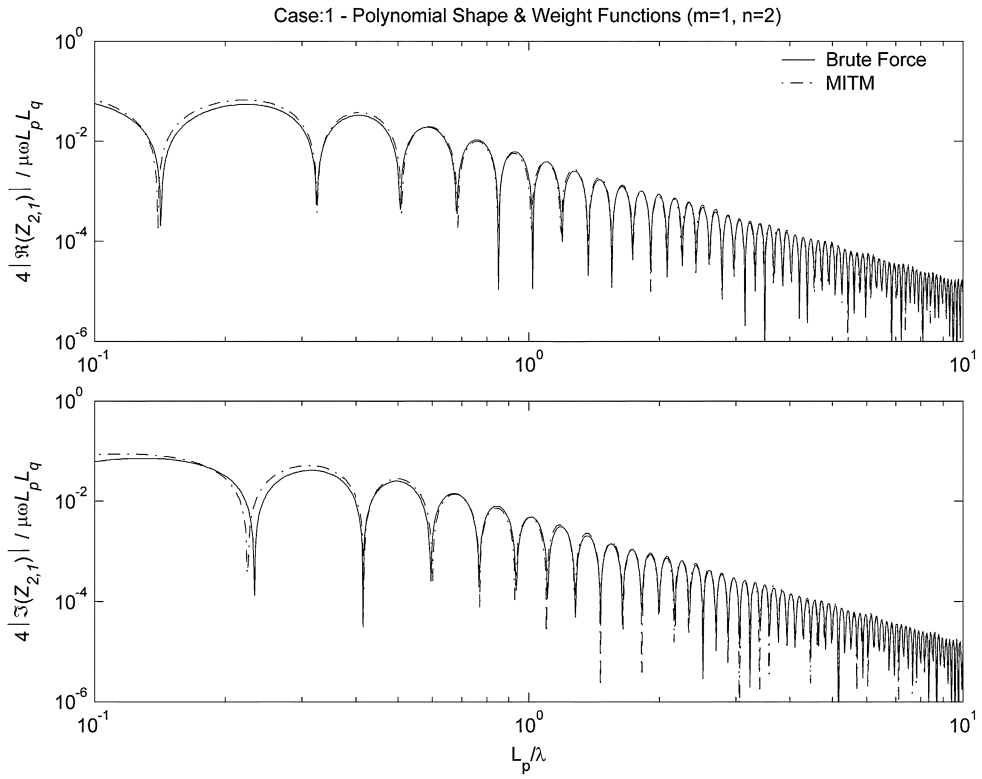

Fig. 2. Numerical evaluation of impedances for `Case 1` (distinct elements) with polynomial shape and weight functions ($m = 1$ and $n = 2$). The solid line is the brute force calculation of (8) and the dashed line is the MITM calculation (16). The impedance is scaled by $4/\mu\omega L_p L_q$.

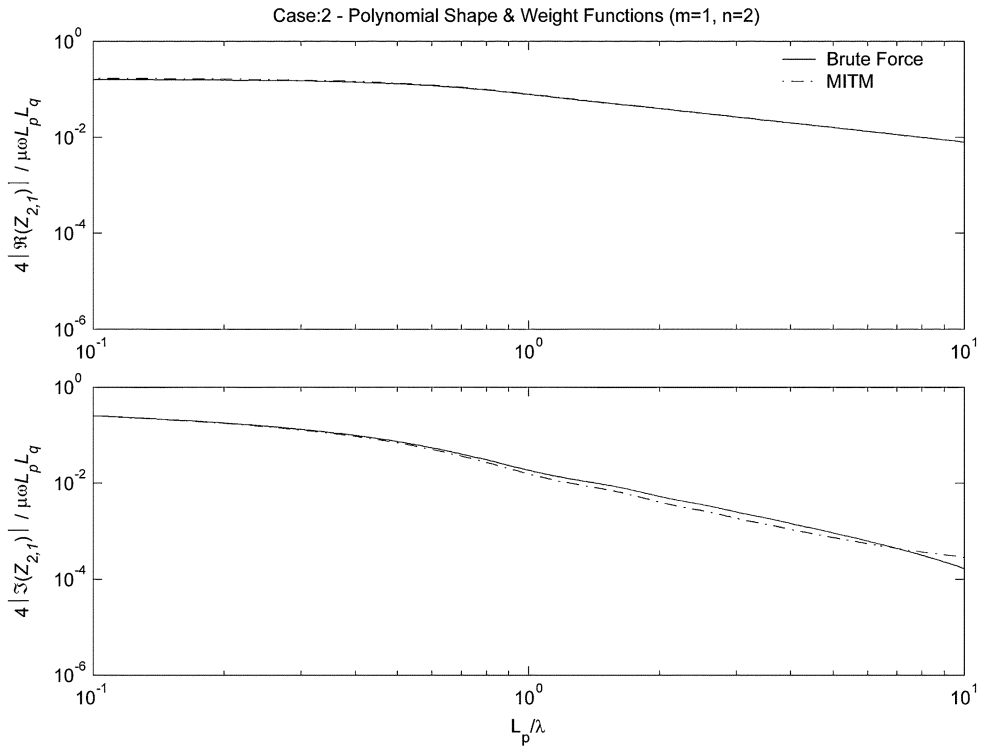

Fig. 3. Numerical evaluation of impedances for `Case 2` (self-element) with polynomial shape and weight functions for ($m = 1$ and $n = 2$). The solid line is the brute force calculation of (8) and the dashed line is the MITM calculation (27). The impedance is scaled by $4/\mu\omega L_p^2$.

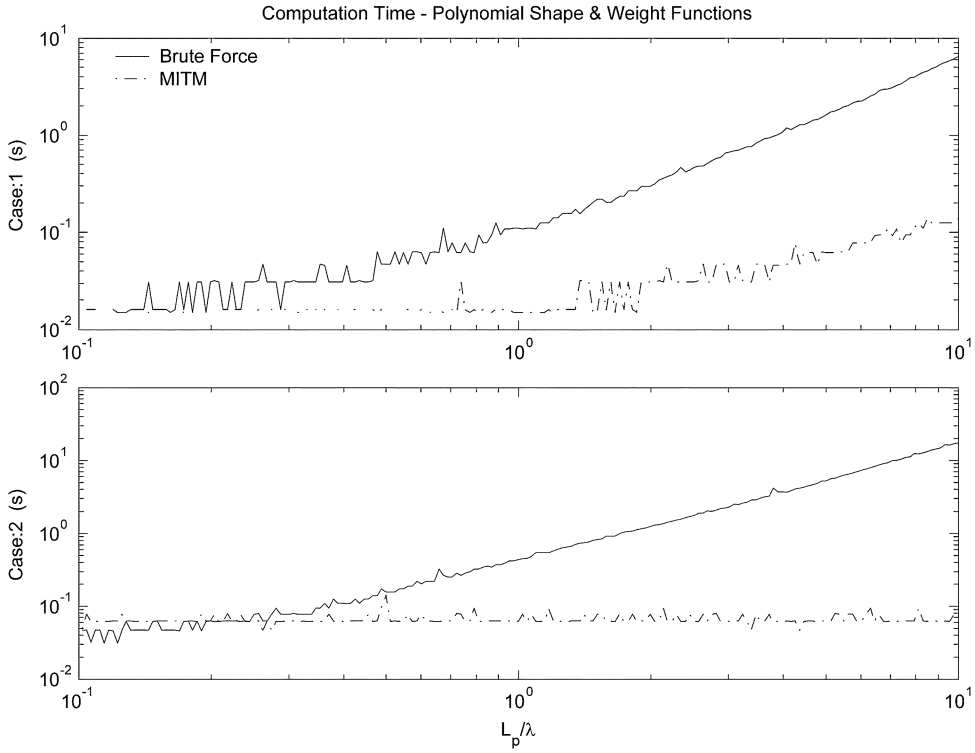

Fig. 4. Computation times for `Case 1` (distinct element) and `Case 2` (self-element). Calculations were performed using MatLab R13 on a 2.4 GHz PentiumIV with 1.0 Gb of RAM.

Note that evaluation of the self-element impedance using (16) does *not* yield the correct results for this function set.

B. Computational Complexity

The computation times for `Case 1` and `Case 2` are presented in Fig. 4. The computational complexity of evaluating (8) via brute force is $N_{bf}\mathcal{O}(40L^*/\lambda)^2$, where N_{bf} is the number of function evaluations for each sample point and $L^* = \sqrt{L_pL_q}$. Because (8) involves a double integral, the computational complexity grows as the *square* of the wave number. For the MITM, the computation complexity is $N_{\mathrm{MITM}}\mathcal{O}(40L^*/\lambda)$, where N_{MITM} is the number of function evaluations at each sample point. For the MITM, this is a *linear* function of the wave number. As the elements become much larger than a wavelength, the brute force method becomes increasingly less efficient than the MITM.

VI. Conclusion

While much attention has been given toward reducing the number of elements in the MoM impedance matrix, there has been little effort made to reduce the matrix fill time. Fill time for the 2-D MoM impedance matrix is a significant burden because the matrix elements are expressed as a double integral. Previous attempts to reduce the matrix fill time utilized approximations of the spectral domain Green's functions [1]–[3] or used approximations of the spatial domain Green's function [4].

This paper presents a generalized process that reduces the fill time of the MoM impedance matrix for a wide range of shape and weight function sets. This is accomplished by using an integral transform that analytically reduces the general, 2-D MoM impedance (8) into a single integral (16), (22) for any shape and weight function set that can be analytically integrated with a complex exponential over the domain [0, 1]. This exact simplification reduces the MoM impedance matrix fill time. The resulting single integrals, though infinite, converge rapidly for polynomial function sets and allow the MoM impedance matrix to be populated much quicker than with the brute force integration.

This method is applicable to both radiation and scattering problems in 2-D electromagnetics and acoustics. In particular, this method is well suited for 2-D radar cross-section calculations of large, PEC structures.

A. Summary of the Moments via Integral Transform Method

By utilizing the $\mathcal{R}$ transformation (13) of the shape and weight functions, the $p \neq q$ impedance terms (8) analytically reduce from double integrals into the MITM contour integral (16). This simplification is possible whenever the transformed shape and weight functions are expressible in a closed form. Similarly, the self-element terms $(p = q)$ reduce into the contour integral (22). Additionally, the proposed method allows shape and weight function sets to be mixed (e.g., polynomial or Fourier sets for large elements and pulse shape/point matching sets for small elements). By mixing the function sets, larger elements $(\lambda > L)$ can benefit from the speed and accuracy of (16) while the smaller elements $(\lambda \cong L/20)$ accurately mesh the scatterers curved regions.

Finally, the transformed function $\mathbf{S}_{pm}$ in (17) and (18) depends only on the mth mode on the pth element; similarly with $\mathbf{W}_{qn}$. Therefore, these functions only need to be tabulated once because the integrand functions $\mathbf{I}^{(1)}_{qn,pm}[u]$ and $\mathbf{I}^{(2)}_{qn,pm}[u]$ are combinations of the transformed functions $\mathbf{S}_{pm}$ and $\mathbf{W}_{qn}$.

ACKNOWLEDGMENT

The authors are grateful to the anonomous reviewers whose comments resulted in an improved paper.

REFERENCES

[1] D. T. DiPerna and D. Feit, "An approximate analytic solution for the radiation from a line-driven fluid-loaded plate," *J. Acoust. Soc. Amer.*, vol. 110, no. 6, pp. 3018–3024, Dec. 2001.

[2] M. I. Aksun, F. Çalişkan, and L. Gürel, "An efficient method for electromagnetic characterization of 2-D geometries in stratified media," *IEEE Trans. Microwave Theory Tech.*, vol. 50, pp. 1264–1274, May 2002.

[3] D. L. Heckmann and S. L. Dvorak, "Novel closed-form expressions for MoM impedance matrix elements for numerical modeling of shielded passive components," *IEEE Trans. Magn.*, vol. 35, pp. 1534–1537, May 1999.

[4] L. Alatan, M. I. Aksun, K. Mahadevan, and M. T. Birand, "Analytical evaluation of the MoM matrix elements," *IEEE Trans. Microwave Theory Tech.*, vol. 44, pp. 519–525, Apr. 1996.

[5] N. Morita, N. Kumagai, and J. R. Mautz, *Integral Equation Methods for Electromagnetics*. Boston, MA: Artech House, 1990, pp. 149–151 and 236–288.

[6] A. Erdélyi, W. Magnus, F. Oberhettinger, and F. G. Tricomi, *Tables of Integral Transforms*. New York: McGraw-Hill, 1954, vol. 1.

[7] I. S. Gradshteyn and I. M. Ryzhik, *Table of Integrals, Series, and Products*. San Diego, CA: Academic, 1980.

[8] F. W. Byron Jr. and R. W. Fuller, *Mathematics of Classical and Quantum Physics*. New York: Dover, 1992, pp. 312–330.

[9] Y. Zhang, "High frequency electromagnetic scattering model of ship–sea surface interactions," Office of Naval Research Rep., Contract N00014-01-F-0102, 2002.

[10] *Schaum's Mathematical Handbook of Formulas and Tables*, McGraw-Hill, New York, 1991, p. 36.

[11] J. D. Hoffman, *Numerical Methods for Engineers and Scientists*. New York: McGraw-Hill, 1992, pp. 191–193.

Jerry R. Smith, Jr. (M'03) received the B.S. degree in physics from Georgia Southern University, Statesboro, in 1994, the M.S. degree in mechanical engineering from The Georgia Institute of Technology, Altanta, in 1996, and the M.S. degree in oceanic engineering from the Virginia Polytechnic Institute and State University, Blacksburg, in 2000. He is currently working toward the Ph.D. degree in electrical engineering at The Catholic University of America, Washington, DC.

He is with the RF Technologies Branch of the Naval Surface Warfare Center, Carderock Division, West Bethesda, MD. His current research efforts focus on modeling techniques and sea scattering phenomena.

Mark S. Mirotznik (M'91) received the B.S.E.E. degree from Bradley University, Peoria, IL, in 1998 and the M.S.E.E., M.S.B.E., and Ph.D. degrees from The University of Pennsylvania, Philadelphia, in 1991 and 1992, respectively.

He is an Associate Professor of electrical engineering at The Catholic University of America, Washington, DC. His research interests include computational electromagnetics and optics, bioelectromagnetics, and biomedical instrumentation.